Virology 527 (2019) 132–140

Contents lists available at ScienceDirect

Virology

journal homepage: www.elsevier.com/locate/virology

Lectin microarray analyses reveal host cell-specific glycan profiles of the hemagglutinins of influenza A viruses

Takahiro Hiono[a,*], Atsushi Matsuda[b], Takanori Wagatsuma[a,c], Masatoshi Okamatsu[d], Yoshihiro Sakoda[d], Atsushi Kuno[a,*]

[a] Glycoscience & Glycotechnology Research Group, Biotechnology Research Institute for Drug Discovery, National Institute of Advanced Industrial Science & Technology, Tsukuba, Ibaraki 305-8568, Japan
[b] Department of Biochemistry, School of Medicine, Keio University, Shinanomachi, Shinjuku-ku, Tokyo 160-8582, Japan
[c] Project for Utilizing Glycans in the Development of Innovative Drug Discovery Technologies, Japan Bioindustry Association (JBA), Hatchobori, Chuo-ku, Tokyo 104-0032, Japan
[d] Laboratory of Microbiology, Department of Disease Control, Faculty of Veterinary Medicine, Hokkaido University, Sapporo 060-0818, Japan

ARTICLE INFO

Keywords:
Influenza A virus
Lectin microarray
Hemagglutinin
Glycosylation
α-Gal

ABSTRACT

Glycan structures on hemagglutinin (HA) of influenza A viruses have been analyzed previously to understand their significance. However, the formerly established methods using mass spectrometry present disadvantages such as procedure complexity, sensitivity, and throughput. Our study has established a novel method for analyzing glycan profiles of HA using lectin microarray techniques. We successfully obtained glycan profiles of HA starting from 1 ml of the 10^6 $TCID_{50}$ samples through simple antigen enrichment using optimized immunoprecipitation. The profiles were reasonably consistent with known glycan structures of HA. Next, we compared glycan profiles of the HAs prepared from chicken embryos, MDCK, Vero, and A549 cells, and demonstrated the host cell-specific HA glycan profiles. Notably, the HA from MDCK cells was α1–3 galactosylated. Our method provides a highly sensitive and simple procedure for glycan profiling of the viral glycoproteins, thereby paving way for direct glycan analyses of human- and animal-derived virions.

1. Introduction

Influenza A virus (IAV) belongs to the family *Orthomyxoviridae*, genus *Alphainfluenzavirus* (King et al., 2018). The virion of IAV is covered with a host cell-derived envelope and three viral proteins, i.e., hemagglutinin (HA), neuraminidase (NA), and M2 ion channel. Of these, HA and NA are glycoproteins. Since HA is the major protein on the envelope, it is mainly targeted by host humoral immunity.

N-glycosylation of the HA modulates the host range, pathogenicity, and immunogenicity of IAVs. Interestingly, the number of *N*-glycosylation sites on the globular head domain of HA in human IAVs has progressively increased since they were first introduced into the human population (Igarashi et al., 2008; Wu and Wilson, 2017). For instance, the globular head of a 1968 isolate, A/Hong Kong/1/1968 (H3N2) possesses only two potential *N*-glycosylation sites at Asn 81 and Asn 165. Although the Asn-X-Ser/Thr sequon motif at position 81 disappeared soon after, H3 HAs have acquired six to seven additional *N*-glycosylation sites on their globular head domain during the past half-century. The biological significance of this phenomenon is explained by the immune evasion from the host humoral immunity (Tate et al., 2014). In other words, the oligosaccharides attached to HA shield the antigenic sites, inhibiting the recognition by antibodies. Besides, stepwise acquisitions of *N*-glycosylation sites in H3N2 viruses attenuated their pathogenicity in mice. On the other hand, an increase or decrease in pathogenicity and transmissibility in chickens has been observed in H5N1 clade 2.2.1.1 viruses (Abdelwhab et al., 2016; Vigerust et al., 2007). It is known that the surfactant protein D (SP-D) is a soluble lectin, which behaves as an antiviral component in the respiratory tract (Hartshorn, 2010). SP-D has the ability to recognize high-mannose type glycans attached on the viral envelope proteins, directly neutralizes the virus infectivity, and induces innate immunity. The *N*-glycosylation of H3 HA at Asn 165 and Asn 246, where high-mannose glycans are attached, is essential for the sensitivity towards neutralization by mouse bronchoalveolar lavage fluid (BALF), which is a good source of SP-D (Tate et al., 2011). In agreement with this, mutant viruses lacking *N*-glycosylation sites at these positions showed higher pathogenicity than the wild-type strain in mice. Moreover, the glycan composition of the HA also affects its immunogenicity. It has been demonstrated

* Corresponding authors.
E-mail addresses: t.hiono@aist.go.jp (T. Hiono), atsu-kuno@aist.go.jp (A. Kuno).

https://doi.org/10.1016/j.virol.2018.11.010
Received 15 October 2018; Received in revised form 16 November 2018; Accepted 16 November 2018
Available online 29 November 2018
0042-6822/

previously that mice vaccinated with HA proteins expressed in human embryonic kidney (HEK) 293T cells carrying complex *N*-glycans elicited higher antibody titers than those carrying glycans with terminal mannose moieties expressed in the insect cell line, *N*-acetylglucosaminyltransferase I (GnTI) deficient cell line, or HEK 293T cells treated with a mannosidase inhibitor, kifunensine (de Vries et al., 2012). As a result, analyses of the glycan profile of the HA are needed to reveal the significance of the glycans on HA.

Although *N*-glycosylation sequon of the HA has been well studied, detailed structural analyses of the HA glycans are still limited. The previous studies mainly employed mass spectrometric approaches for this purpose (An et al., 2015; Khatri et al., 2016; She et al., 2017). These studies were able to perform site-specific glycomic analyses of HA using liquid chromatography mass spectrometry (MS) with high accuracy. Their results demonstrated presence of the core-fucosylated complex *N*-glycans terminating with asialo *N*-acetyllactosamine (LacNAc) or high-mannose *N*-glycans on the HA. Especially for H3 HA, *N*-glycosylation sites, i.e., Asn 165 and Asn 246, in particular, were exclusively occupied by high-mannose type *N*-glycans, while the other sites were occupied by a complex, a hybrid or a high-mannose type glycan (An et al., 2015). The major obstacles for the MS-based analyses of the HA glycans are the sensitivity of the analyses and complexity of the procedure. Khatri et al. used up to 60 μg of total viral proteins and She et al. used up to 20 μg of total viral proteins for analyses of HA by MS (Khatri et al., 2016; She et al., 2017). Since standardized purification protocols are available for IAVs, the preparation up to 10–100 μg viral protein is feasible. However, the procedure requires considerable time and is laborious. Moreover, as glycosylation of the viral proteins is implemented by host cell machinery, the structure of the HA glycan might vary depending on the host cell or their internal environment. To understand the biological implication of the glycans on viral pathogenesis, the direct analysis of the human or animal specimens without employing re-proliferation of viruses with tissue-culture systems and the like is pivotal. However, the conventional procedure cannot be applied to these samples, mainly due to incompatibility with poorly purified samples.

To overcome these limitations, we have established lectin microarray technique (Kuno et al., 2005; Zou et al., 2017). Lectin microarray is a highly sensitive process for obtaining glycomic profiles of *N*- and *O*-glycans by detecting interaction of various lectins with targeted samples containing purified or crude glycoproteins. This method does not require release or purification of glycan moieties or even other complex preparation procedures thereby providing a simple platform for glycomic analyses in a high throughput manner. Consequently, lectin microarray is suitable for the detection of glycome differences with biological and clinical significance using clinical specimens such as serum and tissue, although the technology gives less detailed structural information compared to the MS-based approaches. In the present study, we established an easy and highly sensitive method for the glycan profiling of the HA of IAVs using lectin microarray, coupled with the immunoprecipitation-based protein enrichment procedure. We successfully obtained proportional profiles of the HA glycans starting from 1 ml of 10^6 $TCID_{50}$ samples, which drastically improved the assay sensitivity and compatibility. The host cell-specific glycan profiles of the HA have also been demonstrated in the present study.

2. Results

2.1. Establishment of the virus enrichment and lectin microarray procedures

The overview of the experimental procedures for the analysis of the HA glycans has been summarized in Fig. 1. The previous studies mainly used viral samples derived from embryonated chicken eggs (ECEs) for glycomic analyses of HA. Accordingly, we also used infectious allantoic fluid from ECEs to compare the results obtained in the present study and those in the published literature. For this purpose, ECEs were infected with either A/Puerto Rico/8/1934 (PR/8/34) (H1N1) or A/Aichi/2/1968 (Aichi/2/68) (H3N2), and infectious allantoic fluid was harvested. Before the samples were used for glycan profiling, nucleotide sequences of the HA gene of the viruses were confirmed by Sanger sequencing. The sequences were compared with reference sequences obtained from DDBJ/EMBL/GenBank (https://www.ncbi.nlm.nih.gov/genbank/). Differences between their amino acid sequences and the corresponding reference sequences have been summarized in Supplementary Table 1. Following this, the deduced amino acid sequences were subjected to *N*-glycosylation site prediction using NetNGlyc 1.0 Server (http://www.cbs.dtu.dk/services/NetNGlyc/) (Table 1). The number of *N*-glycosylation sequons was 7 for both PR/8/34 (H1N1) and Aichi/2/68 (H3N2). Among these, site 539 of PR/8/34 (H1N1) should theoretically not be glycosylated since the amino acid is located in the cytoplasmic domain (Khatri et al., 2016). Next, formalin-inactivated infectious allantoic fluid of all specimens was diluted to the titer equivalent to 10^6 $TCID_{50}$ and viral antigens were immunoprecipitated using anti-HA monoclonal antibodies. Viral antigens encompassing HA, NP, and M were successfully enriched (Supplementary Fig. 1). A portion of the immunoprecipitated samples was subjected to the lectin microarray analysis. To obtain well-proportioned profiles of the lectin microarray analyses, dilution factors of the samples applied to the array chips were optimized through several trials. Fig. 2 shows typical results of the lectin microarray analysis using PR/8/34 (H1N1) (A) and Aichi/2/68 (H3N2) (B). As IgGs used for immunoprecipitation and antigen detection are also glycoproteins, several lectins including UDA and Jacalin yielded significant signals in negative control samples, in which PBS was used as starting solution instead of allantoic fluids. Although minor differences in glycan profiles were observed between PR/8/34 (H1N1) and Aichi/2/68 (H3N2), three categories of lectins, namely, lectins specific for fucose (AOL, AAL), LacNAc (RCA120, PHA-E, DSA), and high-mannose *N*-glycans (NPA, GNA, HHL), commonly yielded high signal intensities in the assay. In addition to these lectins, LEL (specific for chitin), WFA (terminal *N*-acetylgalactosamine), and WGA (chitin) also exhibited high signals, possibly due to cross-reaction to multiantenary *N*-glycans terminating with LacNAc. Since these results are consistent with the previously known structure of the HA glycans (An et al., 2015; Khatri et al., 2016), we concluded that glycan profiles were properly evaluated in the designed assay.

2.2. Host cell-specific glycosylation profile of the HA of PR/8/34 (H1N1)

To investigate the host cell-specific glycosylation profile of HA of IAVs, enriched antigens of PR/8/34 (H1N1) were also prepared from the infectious supernatants of MDCK, Vero, and A549 cells. The nucleotide sequences of the HA gene of these samples were confirmed before the glycan profiling. Although an amino acid discrepancy was observed between the ECE-derived PR/8/34 (H1N1) and others (T433I; Supplementary Table 1), all the samples retained the six *N*-glycosylation sequons in the HA ectodomain. Each of the samples was then analyzed with the lectin microarray. The results are shown in Fig. 3. In all samples, the overall profiles were characterized by lectins specific for fucose (AOL, AAL), LacNAc (RCA120, PHA-E, DSA), and high-mannose *N*-glycans (NPA, GNA, HHL). On the other hand, the proportions of these three categories were different in each cell. For example, NPA, GNA, and HHL showed comparable signals with RCA120, PHA-E, and DSA in the HA derived from A549 cells, whereas the signals were remarkably low in the MDCK-derived HA. Although UDA yielded significant signals in the negative control samples, we observed slight differences in the signals of chitin-binding lectins, LEL, STL, and UDA. This implies higher prevalence of poly-LacNAc structures in the glycan of the Vero- and A549-derived HAs as well as the ECE-derived HA than in those of the MDCK-derived HA (Itakura et al., 2017; Togayachi et al., 2007). In addition, several lectins including UEA-I, MAL-I, and EEL showed unique reactivity patterns to antigens prepared in different systems. Especially, the MDCK-derived HA showed high to medium

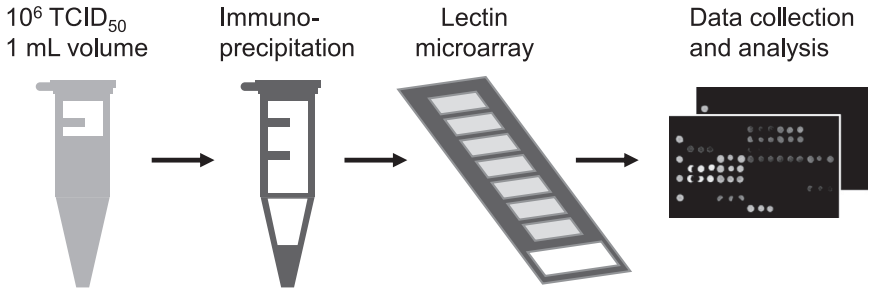

Fig. 1. Overview of experimental procedures. Formalin-inactivated virus solutions were diluted to a titer equivalent to 10^6 $TCID_{50}$ and viral antigens were immunoprecipitated using anti-HA monoclonal antibodies. The antigens were subsequently analyzed by lectin microarray with 45 lectins.

Table 1
Prediction of N-glycosylation sites of the HAs with NetNGlyc 1.0 server.

Strain	Amino acid position[a]	Sequence	Potential	Jury agreement	N-glyc result
PR/8/34 (H1N1)	10	NNST	0.4007	(8/9)	–
	11	NSTD	0.7964	(9/9)	+ + +
	23	NVTV	0.7476	(9/9)	+ +
	268	NASM	0.5349	(5/9)	+
	286	NSSL	0.6421	(9/9)	+ +
	480	NGTY	0.5791	(6/9)	+
	539	NGSL	0.6833	(9/9)	+ +
Aichi/2/68 (H3N2)	8	NSTA	0.8123	(9/9)	+ + +
	22	NGTL	0.7046	(9/9)	+ +
	38	NATE	0.5083	(6/9)	+
	81	NETW	0.5963	(7/9)	+
	165	NVTM	0.7471	(9/9)	+ +
	285	NGSI	0.6789	(9/9)	+ +
	483	NGTY	0.5656	(9/9)	+ +

[a] Numberings are based on matured protein of the HA.

signals in UEA-I and EEL, whereas HA prepared in other cell systems showed considerably lower signals in these lectins. We also evaluated the HA function of the viruses prepared in the different cell systems by their receptor-binding properties (Supplementary Fig. 2). All the samples retain specificity to 3′sialyllactosamine (3′SLacNAc) rather than 6′sialyllactosamine (6′SLacNAc). Although the present results clearly demonstrated the difference of glycan profiles among the HAs prepared in these systems, we could not elucidate any interrelation between the HA function and glycan profiles.

2.3. Changes in the glycome of MDCK cells infected with PR/8/34 (H1N1)

Since the HA prepared in MDCK cells showed unique patterns in the glycan profile using the lectin microarray, we analyzed changes in the glycome of MDCK cells infected with PR/8/34 (H1N1). To achieve this, whole cell lysates of infected or mock-infected MDCK cells were prepared and subjected to the lectin microarray analysis (Fig. 4). The obtained signals were appropriately normalized to conduct one-by-one comparisons of signals for each lectin. The previous studies demonstrated that the mean-normalization is the most preferable for cell lysate samples; therefore, we applied the method for signals normalization (Tateno et al., 2010; Zou et al., 2017). As predicted, changes indicating desialylation, the increases in signals of ECA, RCA120, as well as decrease in the signals of SNA, SSA, and TJA-I were clearly ascertained. In addition, the infection of PR/8/34 (H1N1) induced an increase in the signals of AOL and AAL, which indicates the hyperfucosylation in infected cells. The signals for EEL, which is a specific lectin for MDCK-derived HA, increased upon infection of PR/8/34 (H1N1). On the other hand, changes in UEA-I, another lectin specific for the MDCK-derived HA, were not significant ($P = 0.103$). Accordingly, we focused on glycans recognized by EEL. MDCK cells infected with PR/8/34 (H1N1) were subjected to lectin and immunofluorescence staining using EEL and anti-HA monoclonal antibody (Fig. 5A). Cells stained with the anti-HA antibody were also stained with EEL, whereas anti-HA negative cells were not. Subsequently, whole cell lysates of PR/8/34 (H1N1)- or mock-infected MDCK cells were prepared and resolved with SDS-PAGE followed by EEL based lectin blotting analysis (Fig. 5B). A strong intensity band of approximately 50 kDa was detected in the PR/8/34 (H1N1)-infected sample. Also, the EEL-blotting results, where the lysates were immunoprecipitated with an anti-HA monoclonal antibody, 2F1A7, demonstrate that this EEL-positive glycoprotein is the viral HA (Fig. 5C). These results indicate that glycomic changes associated with EEL recognition were preferentially introduced in the viral HA during infection with PR/8/34 (H1N1).

2.4. α1–3 galactosylation of MDCK-derived HA

To confirm the results of lectin microarray, the majority of the proteins were precipitated from virus solutions prepared in ECEs, MDCK, Vero, and A549 cells using trichloroacetic acid (TCA). Total protein concentrations were roughly quantified by the band intensities for the HA in western blotting and normalized samples were analyzed by EEL lectin blotting (Fig. 6A). Consistent with the results of lectin microarray, we detected a specific band for precipitated proteins from infected MDCK cells. EEL is specific for Galα1–3Gal (α-Gal) epitopes or B antigens of ABO blood group (Teneberg et al., 2003). Since the α1,3-galactosyltransferase encoding gene (for synthesis of α-Gal epitopes) appeared early in mammalian evolution but ceased in humans, apes, and old-world monkeys, endogenous α-Gal epitopes are thus missing in these primates, as well as birds (Galili, 2014; Galili et al., 1988). Accordingly, we hypothesized that these glycan structures recognized by EEL were α-Gal epitopes. To provide evidence for this, viral antigens of PR/8/34 (H1N1) and Aichi/2/68 (H3N2) prepared in either ECEs or MDCK cells were immunoprecipitated with anti-HA antibodies and were probed using the anti-α-Gal antibody in western blotting (Fig. 6B). In H3 HAs, uncleaved HA0 was also detected despite the assay being conducted in reduced conditions, possibly due to the effect of cross-linking by formalin inactivation. Since HA/NP ratios were extremely low in viruses prepared in MDCK cells, only faint bands were detected for the HAs derived from MDCK cells. Nevertheless, when blotted with anti-α-Gal antibody, intense bands were detected in MDCK-derived antigens and the bands were absent in samples prepared in ECEs containing either PR/8/34 (H1N1) or Aichi/2/68 (H3N2). Thus, viral HAs prepared in MDCK cells were α1–3 galactosylated, and the modification was not strain-specific.

3. Discussion

We established a highly sensitive and simple method for glycan profiling of the HA of IAVs using lectin microarray techniques in the present study (Figs. 1 and 2). Using this method, we obtained the glycomic information of the HA starting from 1 ml of 10^6 $TCID_{50}$ samples. Previous studies demonstrated that the HA of IAVs are rich in asialo-,

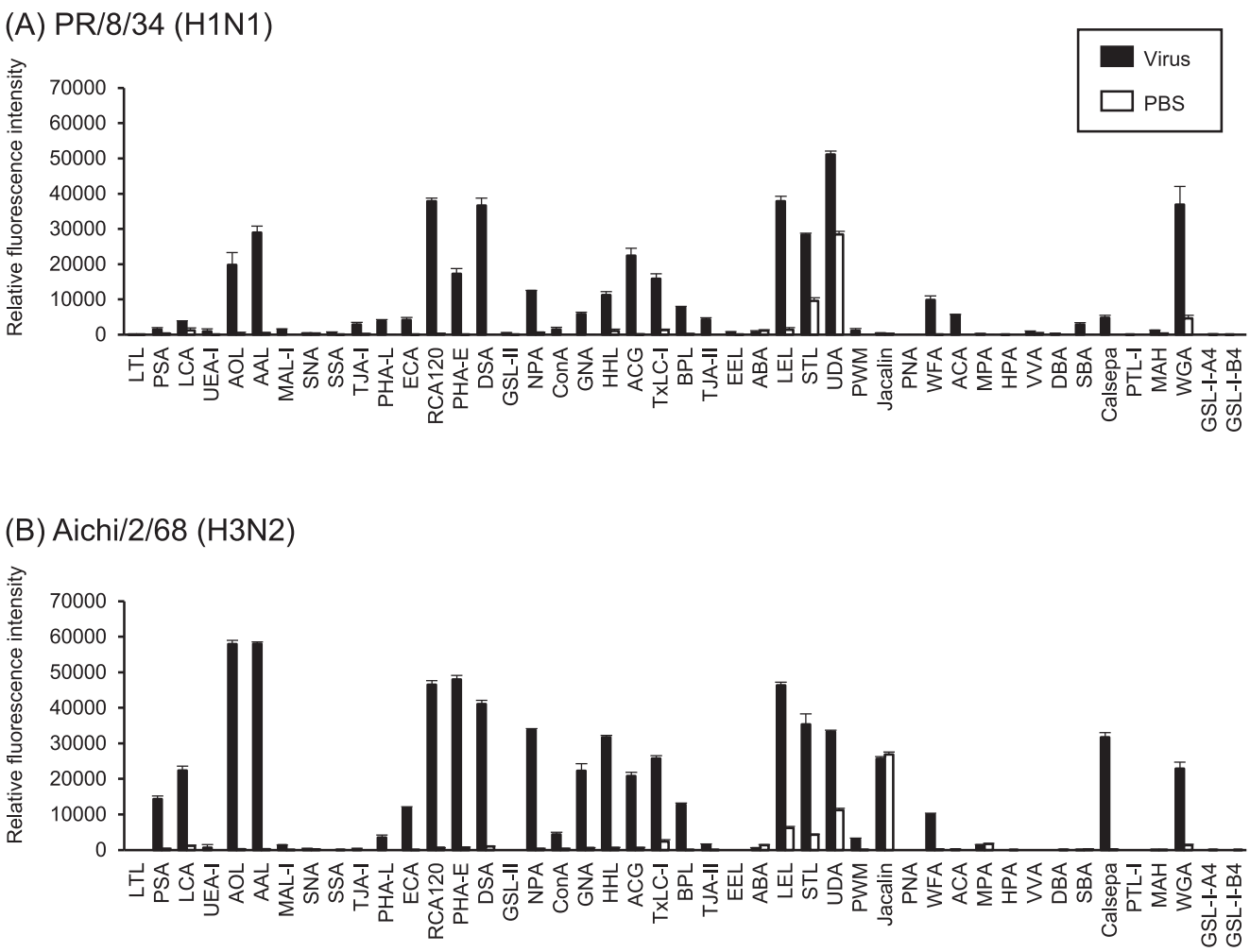

Fig. 2. Glycan profiles of the HA of PR/8/34 (H1N1) (A) and Aichi/2/68 (H3N2) (B) derived from ECEs. Virus antigens (closed bars) or PBS (open bars) were immunoprecipitated using anti-HA monoclonal antibodies and analyzed by lectin microarray with 45 lectins. Data are represented as mean signals of three spots ± standard deviations (SD). PBS was used as starting solution instead of virus solutions so as to evaluate the lectin microarray signals derived from the antibodies used for the immunoprecipitation and antigen detection.

core-fucosylated complex *N*-glycans, and high-mannose *N*-glycans (An et al., 2015; Khatri et al., 2016). Consistent with this, lectins specific for fucose-moieties (AOL, AAL), LacNAc (RCA120, PHA-E, DSA), and high-mannose *N*-glycans (NPA, GNA, HHL) showed higher signal intensity in the lectin microarray, although host cell-dependent differences were observed.

The present method enabled us to conduct a comparative analysis of glycomes of the HA of IAVs that were prepared in different host cells (Fig. 3). These cells, ECEs, MDCK, Vero, and A549 cells, are the most frequently used in the isolation and propagation of IAVs. It was noteworthy that the HA of PR/8/34 (H1N1) prepared in MDCK cells possessed glycans recognized by EEL (Fig. 3) and carried α-Gal epitopes (Fig. 6). The interaction of EEL with MDCK-derived IAVs, and even the presence of the α-Gal epitopes on the virions from MDCK cells, has been previously shown by lectin blotting, lectin affinity chromatography (Opitz et al., 2008, 2007), and liquid chromatography-based structural analysis (Yagi et al., 2012). Previous investigations have also demonstrated that the recombinant HAs or virus-like particles that were artificially α1–3 galactosylated elicited stronger immunity than naturally glycosylated antigens (W. Chen et al., 2017; W.A. Chen et al., 2017). Since humans, apes, and old-world monkeys lack the functional α1,3-galactosyltransferase gene required for the synthesis of α-Gal epitopes, they have natural antibodies against these epitopes (Reviewed in Galili, 2014). Accordingly, α-Gal epitopes are immunogenic in humans. As the anti-α-Gal antibody is the most abundant antibody in the human circulatory systems, it immediately opsonizes α1–3 galactosylated antigens and leads efficient antigen presentations via Fcγ receptors on antigen-presenting cells (W. Chen et al., 2017; W.A. Chen et al., 2017). On the other hand, α-Gal epitopes are known to act as allergens. Hypersensitivity to α-Gal epitopes was first recognized in using Cetuximab, a chimeric mouse-human IgG1 monoclonal antibody against the epidermal growth factor receptor (EGFR), which is used in the treatment of metastatic colorectal cancer and squamous cell carcinoma (Chung et al., 2008). In addition, tick-bite has been shown to induce allergy to α-Gal epitopes, which is associated with a mammalian meat allergy (Van Nunen et al., 2009). It is unclear whether MDCK cell-derived IAVs induce IgE responses against α-Gal epitopes. To the best of our knowledge, there is still no report of the adverse event in MDCK-derived influenza vaccine associated with allergy to α-Gal epitopes, although MDCK-derived influenza vaccines are already approved by the European Medicines Agency Evaluation of Medicines for Human Use and the US Food and Drug Administration (Manini et al., 2016). Hence, safety of the MDCK cell-derived influenza vaccine should be carefully re-evaluated as related to allergic reactions to glycan epitopes.

It is of interest that virus infection induced α1–3 galactosylation in MDCK cells, whereas non-infected MDCK cells were poorly stained by EEL (Figs. 4 and 5). Since NA of IAVs cleaves terminal sialic acid moieties from penultimate galactoses, it is expected that an increase in

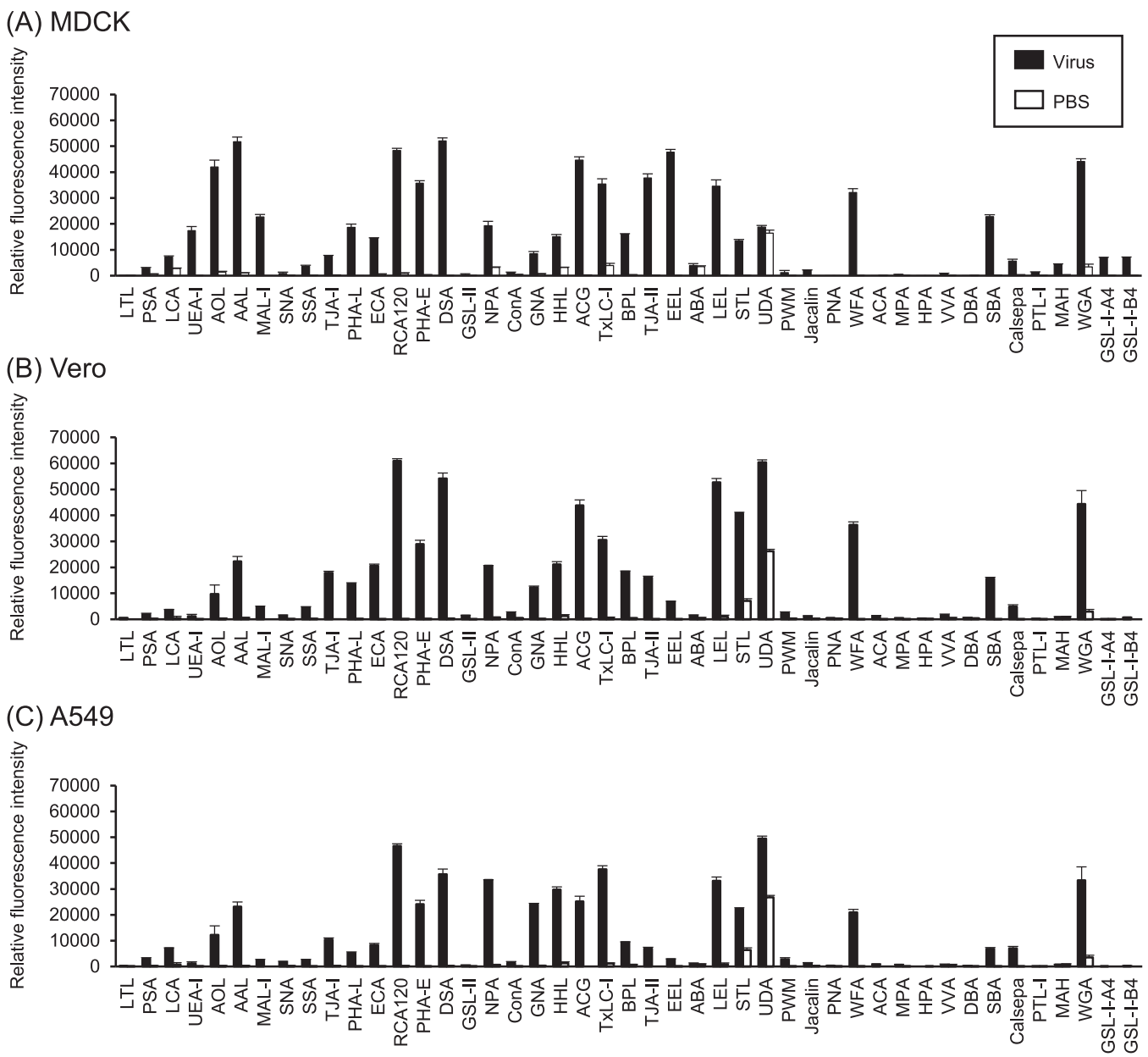

Fig. 3. Glycan profiles of the HA of PR/8/34 (H1N1) derived from MDCK (A), Vero (B), or A549 cells (C). Virus antigens (closed bars) or PBS (open bars) were immunoprecipitated using anti-HA monoclonal antibodies and analyzed by lectin microarray with 45 lectins. Data are represented as mean signals of three spots ± standard deviations (SD). PBS was used as starting solution instead of virus solutions so as to evaluate the lectin microarray signals derived from the antibodies used for the immunoprecipitation and antigen detection.

terminal LacNAc and decrease in sialic acids would be observed in infected cells. In addition, lectin microarray analyses of infected MDCK cells demonstrated not only desialylation, but also other changes such as α1–3 galactosylation and hyperfucosylation of the glycan (Fig. 4). The previous study demonstrated that Herpes simplex virus type-1 (HSV-1) infection upregulated FUT3, FUT5, and FUT6 genes via the NFκB signaling pathway (Nordén et al., 2017). Further, varicella-zoster virus (VZV) and cytomegalovirus (CMV) induced transcriptional activation of multiple fucosyltransferase genes during infection (Nyström et al., 2007). Here, we propose two hypotheses that explain the alteration of glycomes in MDCK cells infected with IAVs. One is that IAVs also induce specific glycosyltransferase genes as do HSV-1, VZV, and CMV. The other is that the desialylation by viral NAs impacts the balance of the global glycome, thereby alternatively inducing α1–3 galactosylation and fucosylation without activating specific glycosyltransferase genes. Especially for the α1–3 galactosylation in the nonreducing terminal, the simplest explanation is that the hydrolysis of sialoside with the NA enable α1–3 galactosyltransferase in MDCK cells to transfer galactose moieties to denuded LacNAc structure. If the increase of α-Gal epitopes is regulated by such mechanisms, this indicates that the viral NA is matured and active in Golgi cisterna, to which the α1–3 galactosyltransferase is localized (Fullmer et al., 2007). In addition, the fact that the HA was preferably α1–3 galactosylated in infected MDCK cells implies the presence of unknown mechanisms that specifically regulate glycan modification of the HA. Thus, the present study significantly contributed to the better understandings of the maturation of both HA and NA. The transcriptomic analyses of glycogenes as well as fine analyses of the localization of viral glycoproteins and glycosyltransferases should unveil the underlying mechanisms and the biological significance of these glycomic changes during IAV infections.

We emphasize that the method established in the present study does not require density gradient ultracentrifugation-based virus purification

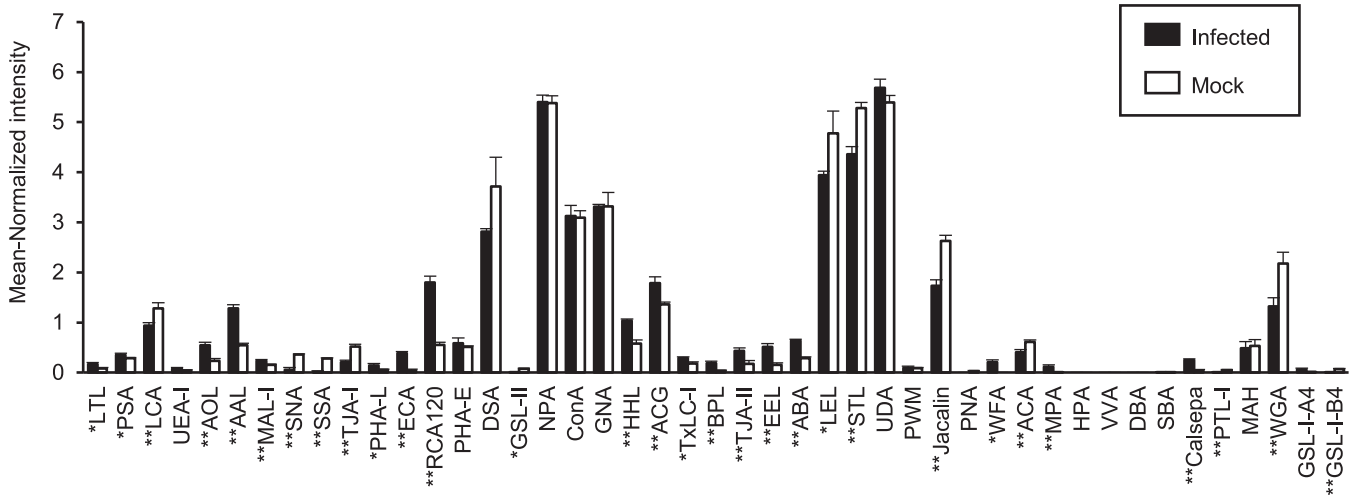

Fig. 4. Glycan profiles of the whole cell lysates of PR/8/34 (H1N1)-infected MDCK cells (closed bars) or mock-infection control (open bars). The data are mean-normalized and represented as mean signals of three biological replicates ± standard deviations (SD). *: $p < 0.05$. **: $p < 0.01$.

(Fig. 1). The high sensitivity and assay compatibility to poorly purified samples were supported by the antibody-overlay protocol of the lectin microarray analysis and a highly sensitive evanescent-field fluorescence-assisted array scanner system. Several studies previously utilized the lectin microarray techniques for glycomic analysis of the Dengue virus (Lei et al., 2015), H9N2 IAV (W. Chen et al., 2017; W.A. Chen et al., 2017), or Hepatitis C virus (Guo et al., 2018), all of which employed density gradient ultracentrifugation for the sample preparation. Only one study succeeded to analyze the glycome of Hepatitis B viruses in 2.5 μl of spiked human serum, which containing 250 ng (0.1 mg/ml) of viral antigens, using almost the same strategy as the present study (Wagatsuma et al., 2018). Although lectin microarray does not provide detailed structural information on glycans, the method established in the present study offers significant advantages in the assay throughput and sensitivity compared with previously suggested methods. In addition, the simple method enables easy access to glycomic analysis in the field of virology. Especially, our method is useful to monitor glycomes of vaccine antigens to avoid undesirable glycan epitopes on the antigens. The glycans attached on the viral glycoproteins are pivotal in that these glycans are involved in the function and structure of the protein as well as the host-pathogen interaction via glycans. Thus, our method in combination with MS-based analyses should contribute to a better understanding of the significance of glycans in viral pathogenesis. Also, the high sensitivity of the established method can pave way for direct glycan analyses of human- and animal-derived virions.

4. Materials and methods

4.1. Viruses and cells

PR/8/34 (H1N1) and Aichi/2/68 (H3N2) were obtained from the Influenza Virus Library at the Faculty of Veterinary Medicine, Hokkaido University (https://virusdb.czc.hokudai.ac.jp). MDCK cells were maintained in Minimum Essential Medium (MEM; Nissui Pharmaceutical, Tokyo, Japan) supplemented with 1 × GlutaMAX (Thermo Fisher Scientific, Waltham, MA, USA) and 5% fetal bovine serum (Hyclone Laboratories, Logan, UT, USA). Vero cells were maintained in MEM supplemented with 1 × GlutaMAX and 10% EquaFETAL® (AtlasBiologicals, Fort Collins, CO, USA). A549 cells were maintained in Dulbecco's Modified Eagle's Medium (D-MEM; FUJIFILM Wako Pure Chemical, Osaka, Japan) supplemented with 10% fetal bovine serum. ECEs were obtained from a local chicken farm.

4.2. Antibodies and lectins

An anti-H1 HA monoclonal antibody, 2F1A7, was purchased from Sino Biological (11684-MM03; Beijing, China). An anti-H1 HA monoclonal antibody, C179, was purchased from TAKARA BIO (M145; Kusatsu, Shiga, Japan). C179 was purified using the MonoSpin ProG column (GL Sciences, Tokyo, Japan) before use. An anti-H3 HA monoclonal antibody, InA246, was purchased from Novus Biologicals (NB100–73162; Littleton, CO, USA). An anti-H3 HA monoclonal antibody, 30-2F11-F7-A5, was purchased from BIO-RAD (OBT1560; Hercules, CA, USA). These antibodies were biotinylated using the Biotin Labeling Kit-NH2 (Dojindo, Kamimashiki, Kumamoto, Japan). An anti-M1 monoclonal antibody, 02, was purchased from Sino Biological (40010-02). An anti-NP polyclonal antibody was purchased from Sino Biological (40207-T60). Biotinylated EEL was purchased from Vector Laboratories (Burlingame, CA, USA). An anti-alpha Gal polyclonal antibody was purchased from Tokyo Chemical Industry (A3123; Tokyo, Japan). An anti-β-actin monoclonal antibody, AC-15, was purchased from Sigma-Aldrich (A5441; St. Louis, MO, USA).

4.3. Preparation of virus solutions

Confluent monolayers of MDCK, Vero, or A549 cells were inoculated with either PR/8/34 (H1N1) and Aichi/2/68 (H3N2) and maintained at 37 °C, 5% CO_2 atmosphere in the presence of 5 (MDCK), 2 (Vero), or 1 (A549) μg/ml of trypsin acetylated (Sigma Aldrich). At 72 h post-infection, cell supernatants were harvested and centrifuged to remove cell debris. Ten-day-old ECEs were inoculated with either PR/8/34 (H1N1) or Aichi/2/68 (H3N2) and incubated at 35 °C for 48 h. The ECEs were chilled and infectious allantoic fluids were harvested. All virus solutions were titrated by $TCID_{50}$ using MDCK cells as described previously (Hiono et al., 2016). The nucleotide sequences of the HA gene of each sample was confirmed by Sanger sequencing using the BigDye Terminator v3.1 Cycle Sequencing Kit (Thermo Fisher Scientific) and an auto-sequencer 3500 Genetic Analyzer (Thermo Fisher Scientific).

4.4. Prediction of N-glycosylation sites

Prediction of N-glycosylation sites was conducted using the NetNGlyc 1.0 Server (http://www.cbs.dtu.dk/services/NetNGlyc/). Full-length amino acid sequences of the HA of PR/8/34 (H1N1) and Aichi/2/68 (H3N2) were analyzed with default parameters.

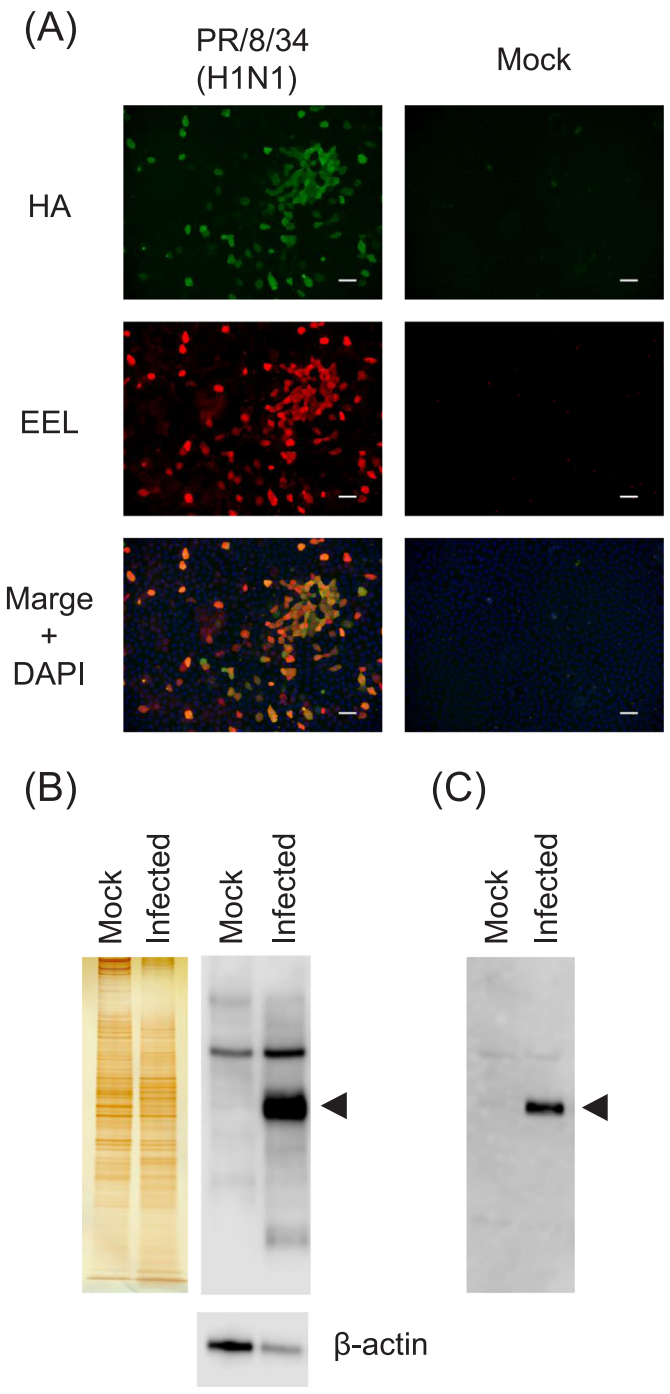

Fig. 5. Glycomic changes associated with EEL recognition were preferentially introduced to the viral HA during PR/8/34 (H1N1) infection. (A) Immunofluorescence and lectin staining of PR/8/34 (H1N1)-infected MDCK cells or mock-infected cells. Cells were stained with the anti-HA monoclonal antibody (green) or EEL (red) and counterstained with DAPI (blue). Bars indicate 50 μm. (B) Whole cell lysates of PR/8/34 (H1N1)-infected MDCK cells or mock-infected control cells were analyzed by SDS-PAGE with silver staining (left), lectin blotting with EEL (top right), or western blotting with the anti-β-actin monoclonal antibody (bottom right). The arrowhead indicates a band with a size of 50 kDa, which is specific for infected cells. (C) Whole cell lysates of PR/8/34 (H1N1)-infected MDCK cells or mock-infected control cells were immunoprecipitated with 2F1A7 and lectin blotted with EEL. The arrowhead indicates a band with a size of 50 kDa, which is specific for infected cells.

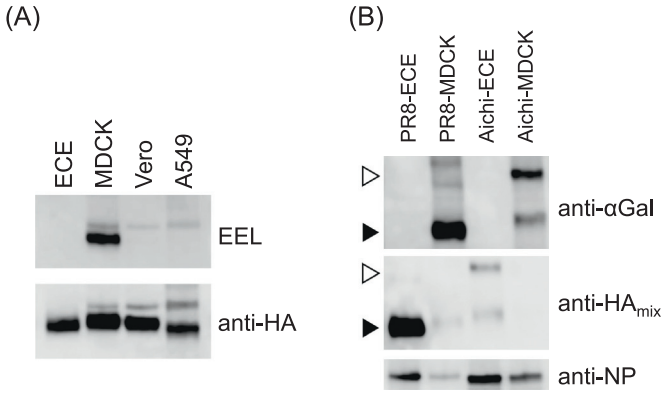

Fig. 6. The α1–3 galactosylation of the HA prepared with MDCK cells. (A) Whole proteins of virus solutions prepared in ECEs, MDCK, Vero, or A549 cells were blotted with EEL or an anti-HA monoclonal antibody. (B) Virus antigens immunoprecipitated with the anti-HA monoclonal antibody were analyzed by western blotting using the anti-α-Gal, anti-NP antibody or mixture of the anti-H1 HA and anti-H3 HA antibodies (anti-HA_{mix}). Open arrowheads indicate uncleaved HA0, and closed arrowheads indicate HA1.

4.5. Immunoprecipitation

Infectious allantoic fluids or cell-culture supernatants containing viruses were inactivated with 0.1% formalin. Subsequently the solution was diluted, and one milliliter of the solution was mixed with 200 ng biotinylated anti-HA monoclonal antibodies. After incubation at 37 °C for 1 h, the complexes were captured with Dynabeads MyOne Streptavidin T1 (Thermo Fisher Scientific) at 4 °C for 1 h. After washing, virus antigens were eluted from magnetic beads and disrupted using 100 mM citric acid containing 1% Triton X-100. Biotinylated antibodies incorporated into the eluted samples were depleted with Dynabeads MyOne Streptavidin T1 at 4 °C for 1 h.

4.6. Lectin microarray

Antibody-overlay lectin microarray was performed as described previously, with some modifications (Kuno et al., 2009). Lectins printed on the array chips are listed in Supplementary Table 2. The glass slides printed with 45 lectins with three replicates (LecChip Ver.1.0; GlycoTechnica, Yokohama, Japan) were activated with probing buffer (Tris-buffered saline containing 1% Triton X-100, 500 mM glycine, 1 mM $CaCl_2$, and 1 mM $MnCl_2$). Immunoprecipitated samples diluted with probing buffer were then applied to the glass slides and incubated overnight at 20 °C. Subsequently the slides were blocked with 0.3 mg/ml human IgG for 30 min at 20 °C. After removal of unbound samples and IgG by subsequent washing, 6.7 μg/ml biotinylated monoclonal antibodies to the HA were added to the slides and incubated for 1 h at 20 °C. Slides were washed thrice and incubated with 1.7 μg/ml Streptavidin, Alexa Fluor 555 Conjugate (Thermo Fisher Scientific) for 30 min at 20 °C. After washing, the slides were scanned with an evanescent-field excitation fluorescence imager (GlycoStation Reader 1200; GlycoTechnica). The obtained images were quantified using the GlycoStation™ ToolsPro Suite ver.1.5 (GlycoTechnica). The net intensity for each lectin was calculated by the mean value of three spots minus the background.

Lectin microarray analyses of whole cell lysates were also conducted. Confluent monolayers of MDCK cells in 100 mm cell culture dishes were infected with 10^4 $TCID_{50}$ of PR/8/34 (H1N1). At 48 h post infection, the whole cell lysate was harvested using PBS containing 1% NP-40 alternative, 0.5% sodium deoxycholate, 0.1% sodium dodecyl sulfate, and cOmplete Ultra Mini protease inhibitor cocktail (Roche, Basel, Switzerland). After quantifying the protein concentration of each sample using the Micro BCA Protein Assay Kit (Thermo Fisher

Scientific), 200 ng of proteins were labeled with 10 μg of Cy3 NHS Ester Mono-reactive (GE Healthcare, Buckinghamshire, UK) in a 10 μl volume at room temperature (RT) for 1 h. The samples were diluted five times with probing buffer and incubated at RT for 2 h to quench the excess fluorescent. Subsequently, 10 ng of labeled protein was applied to the activated LecChip Ver.1.0 and incubated overnight at 20 °C. The glass slides were successively washed and scanned with a GlycoStation Reader 1200. The obtained images were quantified using the GlycoStation™ ToolsPro Suite ver.1.5. The net intensity for each lectin was calculated by the mean value of three spots minus the background, and the relative intensity of each lectin was normalized by the mean value of all lectins for the sample (Tateno et al., 2010).

4.7. Trichloroacetic acid (TCA) precipitation

Virus solution was mixed with 9:1 vol of TCA and incubated on ice for 30 min to precipitate proteins. After centrifugation at 12,000*g* for 5 min, the pellets were successively washed twice with ice-cold 100% ethanol. The pellets were then dissolved in 1× Laemmli SDS sample buffer (62.5 mM Tris HCl pH 6.8, 2% SDS, 10% Glycerol, 0.01% bromophenol blue, 5% β-mercaptoethanol).

4.8. SDS-PAGE, western blot, lectin blot analysis, and silver staining

SDS-PAGE was conducted using a 10–20% gradient polyacrylamide gel (Super Sep Ace, Wako Pure Chemicals, Osaka, Japan) under reducing conditions. The resolved proteins were transferred to Immun-Blot PVDF (BIO-RAD, Hercules, CA, USA). The membrane was blocked with the PVDF Blocking Reagent for Can Get Signal (TOYOBO, Osaka, Japan). Subsequently, the membrane was probed with antigen-specific monoclonal or polyclonal antibodies and appropriate secondary antibodies conjugated with horseradish peroxidase. The proteins were detected using a chemiluminescence substrate, ImmunoStar LD (FUJIFILM Wako Pure Chemical). For the lectin blotting, the membrane was blocked with the PVDF Blocking Reagent for Can Get Signal, followed by further blocking with the Streptavidin/Biotin Blocking Kit (Vector Laboratories, Burlingame, CA, USA). Subsequently, the membrane was probed with biotinylated lectins and streptavidin conjugated with horseradish peroxidase. The glycoproteins were detected as described above. To visualize the total protein of the cell lysates, proteins were resolved using a 10–20% gradient polyacrylamide gel, and the gel was fixed for the conventional silver staining method.

4.9. Solid-phase glycan binding assay

The receptor-binding property of viruses was assessed using a solid-phase glycan binding assay with sialylglycopolymers 3′SLacNAc-polyacrylamide (PAA) and 6′SLacNAc-PAA (GlycoTech, Gaithersburg, MD, USA) as described previously with some modifications (Hiono et al., 2014). Briefly, each sialylglycopolymer was serially diluted and added to each well of a Nunc Immobilizer Amino C8, 96 well strip well microplate (Thermo Fisher Scientific). Each well was blocked with 2% bovine serum albumin (BSA) at room temperature for 2 h. After washing, a solution containing influenza viruses (10^7 $TCID_{50}$/ml in PBS) was added to each well and the plates were incubated at 4 °C for 15 h. After washing, the mouse anti-HA monoclonal antibody was added to each well and the plates were incubated at 4 °C for 2 h. The wells were then washed and incubated with HRP-conjugated secondary antibodies at 4 °C for 2 h. After washing, 100 μl of 1-Step Ultra TMB-ELISA Substrate Solution was added to each well. After incubation at room temperature for 30 min, the reactions were stopped using 50 μl of 2 N H_2SO_4, and the absorbance at 450 nm was measured using a SpectraMax M5 (Molecular Devices, San Jose, CA, USA).

4.10. Immunofluorescence assay and lectin staining of MDCK cells

MDCK cells seeded on the Nunc Lab-Tek II Chamber Slide System (Thermo Fisher Scientific) were infected with IAVs and fixed with cold 100% methanol for 20 h post-inoculation. The cells were stained with anti-HA monoclonal antibodies, Goat anti-Mouse IgG (H + L) Highly Cross-Adsorbed Secondary Antibody, Alexa Fluor Plus 488 (Thermo Fisher Scientific), biotinylated lectins, and Streptavidin Alexa Fluor 555 Conjugate. The glass slides were mounted and counterstained with SlowFade Diamond Antifade Mountant with DAPI (Thermo Fisher Scientific). The fluorescence was visualized using the BZ-X710 (KEYENCE, Osaka, Japan).

Acknowledgements

We thank Dr. Hiroyuki Kaji for invaluable discussions for the work. The present work was supported by Japan Society for the Promotion of Science (JSPS) KAKENHI Grant nos. 16H06597 and 18K15176. The funders had no role in study design, data collection and analysis, decision to publish, or preparation of the manuscript.

Declarations of interest

None.

Appendix A. Supporting information

Supplementary data associated with this article can be found in the online version at doi:10.1016/j.virol.2018.11.010.

References

Abdelwhab, E.S.M., Veits, J., Tauscher, K., Ziller, M., Grund, C., Hassan, M.K., Shaheen, M., Harder, T.C., Teifke, J., Stech, J., Mettenleiter, T.C., 2016. Progressive glycosylation of the haemagglutinin of avian influenza H5N1 modulates virus replication, virulence and chicken-to-chicken transmission without significant impact on antigenic drift. J. Gen. Virol. 97, 3193–3204.

An, Y., McCullers, J.A., Alymova, I., Parsons, L.M., Cipollo, J.F., 2015. Glycosylation analysis of engineered H3N2 influenza A virus hemagglutinins with sequentially added historically relevant glycosylation sites. J. Proteome Res. 14, 3957–3969.

Chen, W., Zhong, Y., Su, R., Qi, H., Deng, W., Sun, Y., Ma, T., Wang, X., Yu, H., Wang, X., Li, Z., 2017a. N-glycan profiles in H9N2 avian influenza viruses from chicken eggs and human embryonic lung fibroblast cells. J. Virol. Methods 249, 10–20.

Chen, W.A., Zhang, J., Hall, K.M., Martin, C.B., Kisselev, S., Dasen, E.J., Vahanian, N.N., Link, C.J., Martin, B.K., 2017b. Addition of αGal HyperAcute™ technology to recombinant avian influenza vaccines induces strong low-dose antibody responses. PLoS One 12, 1–22.

Chung, C.H., Mirakhur, B., Chan, E., Le, Q.-T., Berlin, J., Morse, M., Murphy, B.A., Satinover, S.M., Hosen, J., Mauro, D., Slebos, R.J., Zhou, Q., Gold, D., Hatley, T., Hicklin, D.J., Platts-Mills, T.A.E., 2008. Cetuximab-induced anaphylaxis and IgE specific for galactose-α-1,3-Galactose. N. Engl. J. Med. 358, 1109–1117.

de Vries, R.P., Smit, C.H., de Bruin, E., Rigter, A., de Vries, E., Cornelissen, L.A.H.M., Eggink, D., Chung, N.P.Y., Moore, J.P., Sanders, R.W., Hokke, C.H., Koopmans, M., Rottier, P.J.M., de Haan, C.A.M., 2012. Glycan-dependent immunogenicity of recombinant soluble trimeric hemagglutinin. J. Virol. 86, 11735–11744.

Fullmer, J.H., Riedl, M., Williams, F.G., Sandrin, M., Elde, R., 2007. Enzymes that synthesize the IB4 epitope are not sufficient to impart IB4 binding in dorsal root ganglia of rat. J. Comp. Neurol. 501, 70–82.

Galili, U., 2014. Significance of the evolutionary α1,3-galactosyltransferase (GGTA1) gene inactivation in preventing extinction of apes and old world monkeys. J. Mol. Evol. 80, 1–9.

Galili, U., Shohet, S.B., Kobrin, E., Stults, C.L., Macher, B.A., 1988. Man, apes, and Old World monkeys differ from other mammals in the expression of alpha-galactosyl epitopes on nucleated cells. J. Biol. Chem. 263, 17755–17762.

Guo, Y., Yu, H., Zhong, Y., He, Y., Qin, X., Qin, Y., Zhou, Y., Zhang, P., Zhang, Y., Li, Z., Jia, Z., 2018. Lectin microarray and mass spectrometric analysis of hepatitis C proteins reveals N-linked glycosylation. Medicine 97, e0208.

Hartshorn, K.L., 2010. Role of surfactant protein A and D (SP-A and SP-D) in human antiviral host defense. Front. Biosci. (Schol. Ed.) 2, 527–546.

Hiono, T., Okamatsu, M., Nishihara, S., Takase-Yoden, S., Sakoda, Y., Kida, H., 2014. A chicken influenza virus recognizes fucosylated α2,3 sialoglycan receptors on the epithelial cells lining upper respiratory tracts of chickens. Virology 456–457, 131–138.

Hiono, T., Okamatsu, M., Yamamoto, N., Ogasawara, K., Endo, M., Kuribayashi, S., Shichinohe, S., Motohashi, Y., Chu, D.H., Suzuki, M., Ichikawa, T., Nishi, T., Abe, Y., Matsuno, K., Tanaka, K., Tanigawa, T., Kida, H., Sakoda, Y., 2016. Experimental

infection of highly and low pathogenic avian influenza viruses to chickens, ducks, tree sparrows, jungle crows, and black rats for the evaluation of their roles in virus transmission. Vet. Microbiol. 182, 108–115.
Igarashi, M., Ito, K., Kida, H., Takada, A., 2008. Genetically destined potentials for N-linked glycosylation of influenza virus hemagglutinin. Virology 376, 323–329.
Itakura, Y., Nakamura-Tsuruta, S., Kominami, J., Tateno, H., Hirabayashi, J., 2017. Sugar-binding profiles of chitin-binding lectins from the hevein family: a comprehensive study. Int. J. Mol. Sci. 18.
Khatri, K., Klein, J.A., White, M.R., Grant, O.C., Leymarie, N., Woods, R.J., Hartshorn, K.L., Zaia, J., 2016. Integrated omics and computational glycobiology reveal structural basis for Influenza A Virus glycan microheterogeneity and host interactions. Mol. Cell. Proteom. 15, 1895–1912.
King, A.M.Q., Lefkowitz, E.J., Mushegian, A.R., Adams, M.J., Dutilh, B.E., Gorbalenya, A.E., Harrach, B., Harrison, R.L., Junglen, S., Knowles, N.J., Kropinski, A.M., Krupovic, M., Kuhn, J.H., Nibert, M.L., Rubino, L., Sabanadzovic, S., Sanfaçon, H., Siddell, S.G., Simmonds, P., Varsani, A., Zerbini, F.M., Davison, A.J., 2018. Changes to taxonomy and the International Code of Virus Classification and Nomenclature ratified by the International Committee on Taxonomy of Viruses (2018). Arch. Virol.
Kuno, A., Kato, Y., Matsuda, A., Kaneko, M.K., Ito, H., Amano, K., Chiba, Y., Narimatsu, H., Hirabayashi, J., 2009. Focused differential glycan analysis with the platform antibody-assisted lectin profiling for glycan-related biomarker verification. Mol. Cell. Proteom. 8, 99–108.
Kuno, A., Uchiyama, N., Koseki-Kuno, S., Ebe, Y., Takashima, S., Yamada, M., Hirabayashi, J., 2005. Evanescent-field fluorescence-assisted lectin microarray: a new strategy for glycan profiling. Nat. Methods 2, 851.
Lei, Y., Yu, H., Dong, Y., Yang, J., Ye, W., Wang, Y., Chen, W., Jia, Z., Xu, Z., Li, Z., Zhang, F., 2015. Characterization of N-glycan structures on the surface of mature dengue 2 virus derived from insect cells. PLoS One 10.
Manini, I., Domnich, A., Amicizia, D., Rossi, S., Gasparini, R., Panatto, D., Montomoli, E., Manini, I., Domnich, A., Amicizia, D., Rossi, S., Manini, I., Domnich, A., Amicizia, D., Rossi, S., Pozzi, T., Gasparini, R., Panatto, D., 2016. Flucelvax (Optaflu) for seasonal influenza. Expert Rev. Vaccines 789–804.
Nordén, R., Samuelsson, E., Nyström, K., 2017. NFκB-mediated activation of the cellular FUT3, 5 and 6 gene cluster by herpes simplex virus type 1. Glycobiology 27, 999–1005.
Nyström, K., Grahn, A., Lindh, M., Brytting, M., Mandel, U., Larson, G., Olofsson, S., 2007. Virus-induced transcriptional activation of host FUT genes associated with neo-expression of Leyin cytomegalovirus-infected and sialyl-Lexin varicella-zoster virus-infected diploid human cells. Glycobiology 17, 355–366.
Opitz, L., Salaklang, J., Büttner, H., Reichl, U., Wolff, M.W., 2007. Lectin-affinity chromatography for downstream processing of MDCK cell culture derived human influenza A viruses. Vaccine 25, 939–947.
Opitz, L., Zimmermann, A., Lehmann, S., Genzel, Y., Lübben, H., Reichl, U., Wolff, M.W., 2008. Capture of cell culture-derived influenza virus by lectins: strain independent, but host cell dependent. J. Virol. Methods 154, 61–68.
She, Y.M., Farnsworth, A., Li, X., Cyr, T.D., 2017. Topological N-glycosylation and site-specific N-glycan sulfation of influenza proteins in the highly expressed H1N1 candidate vaccines. Sci. Rep. 7, 1–10.
Tate, M.D., Job, E.R., Brooks, A.G., Reading, P.C., 2011. Glycosylation of the hemagglutinin modulates the sensitivity of H3N2 influenza viruses to innate proteins in airway secretions and virulence in mice. Virology 413, 84–92.
Tate, M.D., Job, E.R., Deng, Y.M., Gunalan, V., Maurer-Stroh, S., Reading, P.C., 2014. Playing hide and seek: how glycosylation of the influenza virus hemagglutinin can modulate the immune response to infection. Viruses 6, 1294–1316.
Tateno, H., Kuno, A., Itakura, Y., Hirabayashi, J., 2010. A versatile technology for cellular glycomics using lectin microarray. Methods in Enzymology 478, 181–195.
Teneberg, S., Alsén, B., Ångström, J., Winter, H.C., Goldstein, I.J., 2003. Studies on Galα3-binding proteins: comparison of the glycosphingolipid binding specificities of Marasmius oreades lectin and Euonymus europeaus lectin. Glycobiology 13, 479–486.
Togayachi, A., Kozono, Y., Ishida, H., Abe, S., Suzuki, N., Tsunoda, Y., Hagiwara, K., Kuno, A., Ohkura, T., Sato, N., Sato, T., Hirabayashi, J., Ikehara, Y., Tachibana, K., Narimatsu, H., 2007. Polylactosamine on glycoproteins influences basal levels of lymphocyte and macrophage activation. Proc. Natl. Acad. Sci. USA 104, 15829–15834.
Van Nunen, S.A., O'Connor, K.S., Clarke, L.R., Boyle, R.X., Fernando, S.L., 2009. An association between tick bite reactions and red meat allergy in humans. Med. J. Aust. 190, 510–511.
Vigerust, D.J., Ulett, K.B., Boyd, K.L., Madsen, J., Hawgood, S., McCullers, J.A., 2007. N-Linked glycosylation attenuates H3N2 Influenza Viruses. J. Virol. 81, 8593–8600.
Wagatsuma, T., Kuno, A., Angata, K., Tajiri, K., Takahashi, J., Korenaga, M., Mizokami, M., Narimatsu, H., 2018. Highly sensitive glycan profiling of Hepatitis B viral particles and a simple method for dane particle enrichment. Anal. Chem. 90, 10196–10203.
Wu, N.C., Wilson, I.A., 2017. A perspective on the structural and functional constraints for immune evasion: insights from Influenza Virus. J. Mol. Biol. 429, 2694–2709.
Yagi, H., Watanabe, S., Suzuki, T., Takahashi, T., Suzuki, Y., Kato, K., 2012. Comparative analyses of N-glycosylation profiles of Influenza A Viruses grown in different host cells. Open Glycosci. 5, 2–12.
Zou, X., Yoshida, M., Nagai-Okatani, C., Iwaki, J., Matsuda, A., Tan, B., Hagiwara, K., Sato, T., Itakura, Y., Noro, E., Kaji, H., Toyoda, M., Zhang, Y., Narimatsu, H., Kuno, A., 2017. A standardized method for lectin microarray-based tissue glycome mapping. Sci. Rep. 7, 1–12.